When the magnetic field is rotated from the [100] direction, site D will have H_x and H_y components and there will be repulsion. Based on the experiment here, the no-field line at 7693.5 Å can be either Γ_1 or Γ_2 of C_{2v}, which are indistinguishable in these experiments, as may be seen from Table I.

III. IDENTIFICATION OF 8128.0- AND 8122.5-Å LINES

Fong's identification of C_s sites is based on six magnetically different orientations for C_s symmetry. The second-order Zeeman effect will thus have six components. However, according to Fong's data only three components each were ever observed for the 8128.0- and 8122.5-Å no-field lines, as shown in Fig. 3. It is clear that his identification is not established. The lines shown in Fig. 3 are not very sharp, but the pattern for 8128.0 Å resembles the calculated pattern for C_{2v} given in Fig. 2(b). (These photos are from the original plates taken by Fong and Wong.[4])

IV. CONCLUSION

The data on the $^7F_3$ lines reported by Fong[6] are not reproducible, and the data obtained in the authors' experiment show there is no justification for C_s symmetry assignment to either the 7693.5- or the 7694.5-Å line. Moreover, the polarization results cannot be explained in terms of the C_s sites as given by Fong for any assumption of the symmetry of the terminal state or transition involved.

As we have shown, the results can be interpreted in terms of the C_{2v} [110] sites. Further evidence that the two lines originate from the same Sm^{2+} ion site will be given in Paper III in this series.

*Work supported in part by National Science Foundation Grant No. GP-6183.

[1]W. E. Bron and W. R. Heller, Phys. Rev. 136, A1433 (1964).
[2]M. Wagner and W. E. Bron, Phys. Rev. 139, A223 (1965).
[3]W. E. Bron, Phys. Rev. 150, A2005 (1965).
[4]F. K. Fong and E. Y. Wong, Phys. Rev. 162, 348 (1967).
[5]F. K. Fong, Phys. Rev. 187, 1099 (1969).
[6]F. K. Fong, Phys. Rev. B1, 4157 (1970).

PHYSICAL REVIEW B VOLUME 4, NUMBER 3 1 AUGUST 1971

Fluorescent Spectra of Sm^{2+} in KCl. II. Site-Symmetry Identification of Prominent Lines in the $^7F_1$ and $^7F_2$ Regions by the Second-Order Zeeman Effect, Including Polarization, Selection Rules, and Intensities*

R. E. Bradbury and E. Y. Wong
Department of Physics, University of California, Los Angeles, California 90024
(Received 26 October 1970)

In a recent publication, Fong and Bellows reported results on high-magnetic-field studies of lines in the low-J-value regions of the fluorescent spectrum of KCl: Sm^{2+} and made site-symmetry assignments accordingly. The authors dispute their methods, data, and identifications on both theoretical and experimental grounds. The authors show that the results of the magnetic field experiments, including both intensity and polarization data as well as splitting, can be interpreted by assigning the prominent lines in these regions as originating from a Sm^{2+} ion in a C_{2v} symmetry site. This is in accord with the earlier work of Bron and Heller.

I. INTRODUCTION

Several years ago, Bron and Heller[1] analyzed the fluorescence spectrum of Sm^{2+} ions in KCl in order to determine the effect on the site symmetry of the Sm^{2+} ion due to the location of the K^+ vacancy which charge compensates the doubly ionized impurity. The method used was that of polarized emission under polarized excitation.[2] Although good polarization data were obtained for the $J=0$, 1, 2, and 3 levels only of the ^7F term, Bron and Heller decided that the prominent spectrum at 10 °K was originating from a C_{2v} nearest-neighbor 110 site. Fong and Wong[3] speculated that other orientations of the K^+ vacancy, leading to correspondingly different site symmetries, should be evidenced in the fluorescent spectrum. Using the first-order Zeeman effect at 4.2 °K with magnetic fields up to 26.5 kG, they found evidence of C_{4v} sites and an axial C_{2v} site, indicating either that the vacancy was further removed from the Sm^{2+} ion or that there simply was an accidental degeneracy. No Zeeman effect was observed in the $J=0$, 1, and 2 regions for the field used, and the two strong lines in the $J=3$ region were not understood. Recently Fong[4] reanalyzed the plates and claimed that the

7694.5-Å line in the $^7F_3$ group originated from ions having C_s site symmetry, and the 7693.5-Å line was of a different symmetry origin. In a previous publication,[5] the authors have shown that the two lines originated from the same ionic site, and the site symmetry responsible is most likely C_{2v}.

Fong[6] performed a theoretical statistical analysis of the Sm^{2+}–K^+-vacancy system in KCl and has been anxious to identify the prominent lines in the spectrum as coming from different sites[4,7] in order to use the intensities to confirm the statistical theories. In Paper III, the authors present evidence independent of the magnetic studies that the prominent lines in the $J \leq 5$ regions, listed in Table I, must originate from the same ion. For the present, we will restrict ourselves to the $J = 1$, 2 regions, with criticism of Fong's identifications in these regions. Fong and his co-workers[7] have better experimental data due to their higher obtainable fields (93.5 kG compared to 67 kG obtainable at UCLA). We have come to entirely different conclusions based on their published data as well as our own. Before giving our criticism of the work of Fong and his co-workers, we will present the theory of the second-order patterns.

II. THEORETICAL DISCUSSION OF SECOND-ORDER ZEEMAN ANISOTROPY PATTERNS

Patterns for the first-order Zeeman effect were discussed by Fong and Wong.[3] Though the second-order effect is straightforward, we present here a detailed discussion in order to illustrate certain points and to define and explain the tables presented. The point symmetries which will be discussed are C_{2v} and C_s, the character tables for these groups being presented in Table II for convenience. The character table of C_{4v} is also presented but will be discussed in the subsequent subsection.

When the crystal is placed in a magnetic field $\vec{H}$, an additional term is added to the Hamiltonian of the Sm^{2+} ion given by

$$\mathcal{H}_m = \vec{\mu} \cdot \vec{H} , \tag{1}$$

where $\vec{\mu}$ is the magnetic dipole moment given by

$$\vec{\mu} = \mu_B \sum_q (\vec{l}_q + 2\vec{s}_q) . \tag{2}$$

μ_B is the Bohr magneton and $\vec{l}_q$, $\vec{s}_q$ are the orbital-angular-momentum and spin operators for electron q. Since the sum over closed shells will yield zero, the sum is taken over the $4f$ electrons in the Sm^{2+} ion only. Nondegenerate states exhibit second- or higher-order Zeeman effect and the multiplicity or splitting of lines is solely due to the multiplicity of sites. The second-order contribution to the energy is given by standard perturbation theory as

$$\Delta\epsilon_a = \sum_{i \neq a} \frac{\langle a|\mathcal{H}_m|i\rangle\langle i|\mathcal{H}_m|a\rangle}{E_a - E_i} , \tag{3}$$

where the sum is over all states $i \neq a$. Major contributions will come from close-lying states, particularly those from the same J manifold. Letting

$$\vec{H} = H_0 \vec{h} , \tag{4}$$

where $\vec{h}$ is a unit vector in the direction of the magnetic field, Eq. (3) can be rewritten

$$\frac{\Delta\epsilon_a}{H_0^2} = \sum_i \frac{\langle a|\vec{h}\cdot\vec{\mu}|i\rangle^2}{E_a - E_i} . \tag{5}$$

If each component of $\vec{\mu}$ transforms like a different irreducible representation of the appropriate group, Eq. (5) can be written as

TABLE I. Summary of the fluorescent lines of KCl: Sm^{2+} in the $J \leq 2$ regions. (s designates the strong or prominent lines in the spectrum.)

Transition region (ΔJ)		Wavelength (Å)	Symmetry assignments: Fong and Bellows (Ref. 7)	Present work	
0→0	s	6891.9	...		...
0→1	s	7014.7	C_{2v}	C_{2v}	Γ_2
		7018.0	C_s	C_s	
		7022.7	C_s	C_s	
	s	7031.7	C_s	C_{2v}	$\Gamma_4(\Gamma_3)$
	s	7048.2	...	C_{2v}	$\Gamma_3(\Gamma_4)$
0→2		7258.0	C_{4v}	C_{2v}	Γ_4
		7263.2	C_s		
	s	7264.4	C_{2v}	C_{2v}	$\Gamma_1(\Gamma_2)$
	s	7282.8	C_{4v}	C_{2v}	$\Gamma_1(\Gamma_2)$
		7284.8	C_{4v}		
		7300.9	C_{4v}		
	s	7304.6	C_{4v}	C_{2v}	Γ_4
	s	7327.8	...	C_{2v}	$\Gamma_2(\Gamma_1)$

$$\frac{\Delta\epsilon_a}{H_0^2}=\sum_\alpha h_\alpha^2 \sum_i \frac{\langle a|\mu_\alpha|i\rangle^2}{E_a-E_i} \quad , \tag{6}$$

where α designates the components in a standard Cartesian coordinate system for the site, appropriate to the point group as given in Table III. For C_{4v} and C_{2v} the z axis is along the axis defined by the K^+ vacancy and the Sm^{2+} ion. The lattice point for the Sm^{2+} will always be taken as 000. If a typical K^+ vacancy site is selected, associated sites may be generated by the operations of O_h, as listed in the second column of Table III. There are twice as many sites as listed, those omitted being related to those listed by the inversion operator. Inclusion of these sites would add nothing new since the second-order effect is invariant to inversion of the magnetic field.

These associated sites are equivalent crystal field sites yielding identical spectra. In a mag-

TABLE II. Character tables of C_s, C_{2v}, and C_{4v}.

C_s	E	σ_h	Base
Γ_1	1	1	x, y, L_z
Γ_2	1	−1	z, L_x, L_y

C_{2v}	E	C_2	σ_v	σ_v'	Base
Γ_1	1	1	1	1	z
Γ_2	1	−1	−1	1	x, L_y
Γ_3	1	1	−1	−1	L_z
Γ_4	1	−1	1	−1	y, L_x

C_{4v}	E	C_4	C_2	σ_v	σ_v'	Base
Γ_1	1	1	1	1	1	z
Γ_2	1	1	1	−1	−1	L_z
Γ_3	1	−1	1	1	−1	
Γ_4	1	−1	1	−1	1	
Γ_5	2	0	−2	0	0	x, y, L_x, L_y

TABLE III. Site field components for C_{2v} and C_s site symmetries with $\vec{H}$ in the (001) plane.

Site Symmetry	K^+ vacancy location	Magnetic site	Site axes (not normalized) x	y	z	Site field components for $\vec{h}=(a,b,0)$ h_x	h_y	h_z
(a) C_{2v}	110	A	$[\bar{1}10]$	[001]	[110]	$-(a-b)/\sqrt{2}$	0	$(a+b)/\sqrt{2}$
	$1\bar{1}0$	B	[110]	[001]	$[1\bar{1}0]$	$-(a+b)/\sqrt{2}$	0	$(a-b)/\sqrt{2}$
	101	C	$[\bar{1}01]$	[010]	[101]	$-a/\sqrt{2}$	b	$a/\sqrt{2}$
	$10\bar{1}$	C	$[\bar{1}0\bar{1}]$	[010]	$[10\bar{1}]$	$-a/\sqrt{2}$	b	$a/\sqrt{2}$
	011	D	$[0\bar{1}1]$	[100]	[011]	$b/\sqrt{2}$	a	$b/\sqrt{2}$
	$01\bar{1}$	D	[011]	[100]	$[01\bar{1}]$	$b/\sqrt{2}$	a	$b/\sqrt{2}$
(b) C_s (I)	211	A	$[0\bar{1}\bar{1}]$	[100]	$[0\bar{1}1]$	$-b/\sqrt{2}$	a	$-b/\sqrt{2}$
	$21\bar{1}$	A	$[0\bar{1}1]$	[100]	$[0\bar{1}\bar{1}]$	$-b/\sqrt{2}$	a	$-b/\sqrt{2}$
	$2\bar{1}1$	B	$[01\bar{1}]$	[100]	[011]	$b/\sqrt{2}$	a	$b/\sqrt{2}$
	$2\bar{1}\bar{1}$	B	[011]	[100]	$[01\bar{1}]$	$b/\sqrt{2}$	a	$b/\sqrt{2}$
	121	C	$[\bar{1}0\bar{1}]$	[010]	$[\bar{1}01]$	$-a/\sqrt{2}$	b	$a/\sqrt{2}$
	$12\bar{1}$	C	$[\bar{1}01]$	[010]	$[\bar{1}0\bar{1}]$	$-a/\sqrt{2}$	b	$a/\sqrt{2}$
	$\bar{1}21$	D	$[10\bar{1}]$	[010]	[101]	$a/\sqrt{2}$	b	$a/\sqrt{2}$
	$\bar{1}2\bar{1}$	D	[101]	[010]	$[10\bar{1}]$	$a/\sqrt{2}$	b	$a/\sqrt{2}$
	112	E	$[\bar{1}\bar{1}0]$	[001]	$[1\bar{1}0]$	$-(a+b)/\sqrt{2}$	0	$(a-b)/\sqrt{2}$
	$\bar{1}\bar{1}2$	E	[110]	[001]	$[\bar{1}10]$	$(a+b)/\sqrt{2}$	0	$(b-a)/\sqrt{2}$
	$\bar{1}12$	F	$[1\bar{1}0]$	[001]	$[\bar{1}\bar{1}0]$	$(a-b)/\sqrt{2}$	0	$-(a+b)/\sqrt{2}$
	$1\bar{1}2$	F	$[\bar{1}10]$	[001]	[110]	$-(a-b)/\sqrt{2}$	0	$(a+b)/\sqrt{2}$
(c) C_s (II)	310	A	[100]	[010]	[001]	a	b	0
	$3\bar{1}0$	B	[100]	$[0\bar{1}0]$	$[00\bar{1}]$	a	$-b$	0
	301	C	[100]	[001]	$[0\bar{1}0]$	a	0	$-b$
	$30\bar{1}$	C	[100]	$[00\bar{1}]$	[010]	a	0	b
	130	D	[010]	[100]	[001]	b	a	0
	$\bar{1}30$	E	[010]	$[\bar{1}00]$	$[00\bar{1}]$	b	$-a$	0
	031	F	[010]	[001]	[100]	b	0	a
	$03\bar{1}$	F	[010]	$[00\bar{1}]$	$[\bar{1}00]$	b	0	$-a$
	013	G	[001]	[010]	[100]	0	$-b$	a
	$0\bar{1}3$	G	[001]	$[0\bar{1}0]$	[100]	0	$-b$	a
	103	H	[001]	$[\bar{1}00]$	$[0\bar{1}0]$	0	$-a$	$-b$
	$\bar{1}03$	H	[001]	[100]	[010]	0	a	b

TABLE IV. Nonzero matrix elements for the operators $\vec{r} = (x, y, z)$ and $\vec{L} = (L_x, L_y, L_z)$ in point group C_{2v} ($\vec{r}$ in upper-left corner, $\vec{L}$ in lower-right).

C_{2v}	Γ_1	Γ_2	Γ_3	Γ_4
Γ_1	z / 0	x / L_y	0 / L_z	y / L_x
Γ_2	x / L_y	z / 0	y / L_x	0 / L_z
Γ_3	0 / L_z	y / L_x	z / 0	x / L_y
Γ_4	y / L_x	0 / L_z	x / L_y	z / 0

netic field, due to different orientations with the magnetic field, the equivalence is reduced. Those sites which are magnetically distinct, i.e., have the same level shift due to the magnetic field, are designated by upper case letters in the third column of Table III.

For dipole radiation the intensity is proportional to the square of the sine of the angle between the dipole moment and the axis of observation. Since the crystal was cleaved, rather than polished, to give normal surface viewing, surface effects preclude intensity discussion when viewed off normal. Specific cases will be discussed in the following.

C_{2v} Symmetry

For the group C_{2v} which arises for a typical K^+ vacancy site at 110, μ_x, μ_y, and μ_z will transform as Γ_2, Γ_3, and Γ_4, respectively, and Eq. (6) can be used. The nonzero matrix elements of $\vec{\mu}$ are the same as those for $\vec{L}$ given in Table IV. The component of $\vec{h}$ and the coordinate axes are listed in Table III, for $\vec{h} = (a, b, 0)$ in the (001) plane with $a = \cos\theta$, $b = \sin\theta$, where θ is the angle between $\vec{h}$ and the [110] direction.

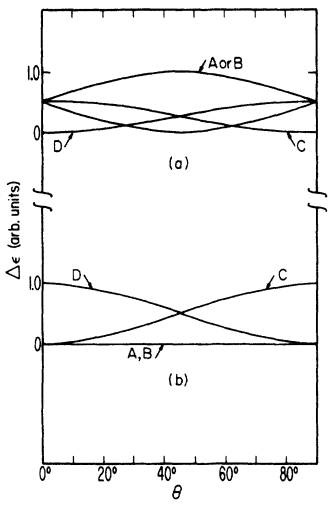

FIG. 1. Second-order Zeeman anisotropy patterns for two-level systems under C_{2v} site symmetry: (a) Γ_1 and Γ_3, Γ_1 and Γ_4, Γ_2 and Γ_3, Γ_2 and Γ_4, (b) Γ_1 and Γ_2 or Γ_3 and Γ_4.

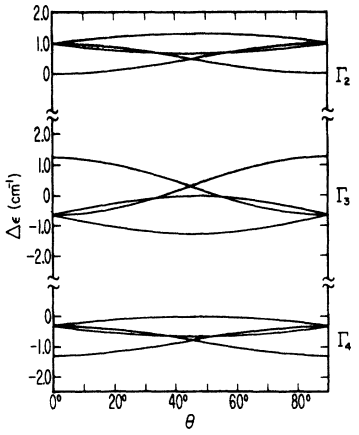

FIG. 2. High-field Zeeman effect for the $J = 1$ manifold of a C_{2v} site calculated from the spin Hamiltonian.

As an example, the second-order Zeeman effect shift for a Γ_2 state of the ion in site C could be written as

$$\frac{\Delta\epsilon(\Gamma_2, C)}{H_0^2} = h_y^2 \sum_i \frac{\langle a|\mu_y|i\rangle^2}{E_a - E_i} + h_x^2 \sum_j \frac{\langle a|\mu_x|j\rangle^2}{E_a - E_j} + h_z^2 \sum_k \frac{\langle a|\mu_z|k\rangle^2}{E_a - E_k} \qquad (7a)$$

$$= \cos^2\theta\, \tfrac{1}{2}(M_{23}^x + M_{24}^z) + \sin^2\theta\, M_{21}^4 \,. \qquad (7b)$$

The shift for site D is obtained merely by exchanging $\cos\theta$ and $\sin\theta$. The definition of M_{23}^x, etc., which are independent of θ, follows by comparison of Eqs. (7a) and (7b). If one state lies much closer to the state in question than all the others, it will dominate the perturbation and permit treatment as a two-level system. For C_{2v}, only the two distinct two-level patterns shown in Fig. 1 can occur. Figure 1(b) comes from either a Γ_1 and Γ_2 or Γ_3 and Γ_4 combination, and Fig. 1(a) comes from the four remaining combinations. Figure 1(b) resembles half of a C_{4v} first-order pattern,[3] except the variation is quadratic in the $H_0\cos\theta$ instead of linear. This illustrates that the anisotropy pattern alone cannot determine the site symmetry and other information such as polarization and intensity must be considered.

The general case is a combination of the two patterns and fitting an individual line requires

TABLE V. Intensities and polarizations for electric dipole transitions in C_{2v} site symmetry from a Γ_1 state to the states indicated with $\vec{H}$ along [100] axis. I_L and I_T are intensities when observed along the [100] and [010] axes, respectively. Polarizations are for observation along the [010] axis. For magnetic dipole transitions, change Γ_1 to Γ_3 and exchange Γ_2 with Γ_4 and π with σ.

Magnetic site	I_L			I_T			Polarization		
	Γ_1	Γ_2	Γ_4	Γ_1	Γ_2	Γ_4	Γ_1	Γ_2	Γ_4
A	$\frac{1}{2}$	$\frac{1}{2}$	1	$\frac{1}{2}$	$\frac{1}{2}$	1	π	π	σ
B	$\frac{1}{2}$	$\frac{1}{2}$	1	$\frac{1}{2}$	$\frac{1}{2}$	1	π	π	σ
(2)C	$\frac{1}{2}$	$\frac{1}{2}$	1	1	1	0	$\pi\sigma$	$\pi\sigma$	...
(2)D	1	1	0	$\frac{1}{2}$	$\frac{1}{2}$	1	σ	σ	π

adjustment of at most three constants. It is far more satisfying and convincing if we are able to make calculations from a spin Hamiltonian in which the constants are adjusted to fit only the zero-field data. For a C_{2v} site, the spin Hamiltonian $S=1$ is[3]

$$\mathcal{H}_s = g\mu_B \vec{H}\cdot\vec{S} + D\,[S_z^2 - \tfrac{1}{3}S(S+1)] + \tfrac{1}{2}E\,[S_+^2 + S_-^2] \quad . \quad (8)$$

Taking the values of $g=1.5$, $D=0$, and $E=34$ cm^{-1}, the patterns shown in Fig. 2 were obtained from Eq. (8). Note that for the Γ_2 state at $\theta=0$, the line from site D remains at the zero-field position. This occurs because Γ_1 is not contained in the $J=1$ manifold. Contributions from levels outside the $J=1$ manifold are not insignificant and interaction with Γ_1 in $J=0$ and $J=2$ levels will shift the line slightly off the zero-field position. The component from site D can be identified accordingly.

When H is along the [100] direction, sites A, B, and C are the same but different from site D so far as the energy shift is concerned. The second-order Zeeman pattern will have two components corresponding to sites A, B, and C and site D. The polarization and intensity of these sites are given in Table V. Intensity for the C_{2v} sites with $\vec{h}$ along the [100] direction may be summarized in the following two rules:

(i) If the two components show equal intensity viewed normal to the magnetic field, then one line (from site D) will be missing when viewed along the field. In this case the lower state will be Γ_4 for electric dipole transition and Γ_2 for magnetic dipole transitions (the upper state is Γ_1 of $^5D_0$).

(ii) If a three-to-one ratio is observed for the two components when viewed normal to the magnetic field, then equal intensity will be observed when viewed along the field. In this case the lower state is either Γ_2 or Γ_1 for electric dipole transition and Γ_3 or Γ_4 for magnetic dipole transition.

C_s Symmetry

Typical K^+ vacancies at 211 and 310 give rise to two distinct C_s symmetries which we will refer to as C_s(I) and C_s(II) following Fong and co-workers. (This group does not enable us to know *a priori* the best choice of x and y axes, although the z axis is determined by the reflection plane. The axes chosen in the table are arbitrary but consistent.) Since μ_x and μ_y both transform like Γ_2, Eq. (7a) cannot be used and the shift will have the general form

$$\frac{\Delta\epsilon_a}{H_0^2} = h_z^2 \sum_{i\neq a} \frac{\langle a|\mu_z|i\rangle^2}{E_a - E_i} + \sum_{j\neq a} \frac{(h_x\langle a|\mu_x|j\rangle + h_y\langle a|\mu_y|j\rangle)^2}{E_a - E_j} . \quad (9)$$

This results in six magnetically distinct sites for C_s(I) and eight for C_s(II). When $\vec{H}$ is along [100], a general line will split into two and three components for C_s(I) and C_s(II), respectively.

If we have a two-level system in C_s(I) in which both levels transform according to the same irreducible representation, they will interact only through μ_z, resulting in a pattern like that shown in Fig. 3(a). If the two levels transform according to different representations, then there will be matrix elements for μ_x and μ_y but none for μ_z. The pattern in Fig. 3(b) was calculated for a two-level system in which $\langle\Gamma_1|\mu_x|\Gamma_2\rangle$ and $\langle\Gamma_1|\mu_y|\Gamma_2\rangle$ are assumed to be equal, though this is not necessarily true. The pattern in Fig. 3(c) was calculated for a three-level system in which the interaction with the same representation was taken to be five times as great as the interaction with the different representation.

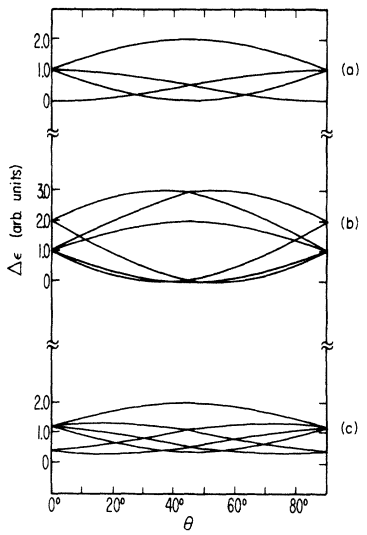

FIG. 3. Second-order Zeeman anisotropy patterns for C_s(I) site symmetry: (a) two-level system, same representation, (b) two-level system, different representations, (c) three-level system. (b) and (c) are not completely general. See text for explanation.

For C_s (II) a two-level interaction between states of the same representation leads to a pattern like Fig. 1(b). The assumption that

$$\langle \Gamma_1 | \mu_x | \Gamma_2 \rangle = \langle \Gamma_1 | \mu_y | \Gamma_2 \rangle \quad (10)$$

leads to additional degeneracy making sites A, B, D, and E equivalent to C, F, G, and H, respectively. This would lead to patterns indistinguishable from the C_{2v} case with only four magnetically distinct sites. We must rely on the selection rules and branching to eliminate this possibility, e.g., under C_s symmetry no transitions are forbidden for either electric or magnetic transitions. The general case in which one of the moments is larger than the other leads to a complex eightfold pattern.

III. CRITIQUE OF WORK OF FONG AND CO-WORKERS

Recent articles by Fong and his co-workers[4,7] have raised many doubts on our part. Our most important objections follow.

a. Induced transitions. Using a magnetic field of 93.5 kG, Fong and Bellows[7] obtained Zeeman shifts of up to 2 cm^{-1} in the $J \leq 2$ regions. The matrix elements between different states of the same J levels or different J levels involving $^7F_0$, $^7F_1$, and $^7F_2$ are about 1.5 $\mu_B H$ or 6.55 cm^{-1} for the field used. For a two-level system, a separation of no more than 40 cm^{-1} would be required to produce a second-order shift of 2 cm^{-1}. In addition to inducing a level shift, the second-order effect also results in a corresponding mixing of wave functions for the two states, which in this case would be about 17%. This mixing will induce transitions if one of the levels is a forbidden transition. Neither the data presented by Fong and Bellows nor those obtained by the present authors show any evidence of induced transitions in this region, though the authors would have observed such transitions even if they were several orders of magnitude lower in intensity than the strong lines. (Induced transitions are observable in other regions.) *The lack of induced transitions implies that all of the interacting states are already observed.* Since the minimum number of states required for the second-order interaction is two, the number of lines observed for each site in each region must be at least two. There cannot be only one C_{2v} site line in both the $^7F_1$ and $^7F_2$ regions as claimed by Fong and Bellows.[7]

Magnetic transitions are allowed from Γ_1 to both the Γ_2 and Γ_5 state of C_{4v} in the $J=1$ manifold (see Table VI). The only state around for the Γ_2 state to interact with would be the Γ_5 state which would show a first-order effect if already observed or would appear as an induced transition if not observed in zero field. Since neither result is observed, we must conclude that though C_{4v} sites do exist in the crystal,[3] they are not responsible for any of the lines observed in the $J=1$ or 2 regions.

b. Confirming data. Fong and Bellows's statement that "optical access perpendicular to the magnetic field was necessary"[7] indicates they are aware that polarization data can be obtained this way although no such data were reported. Fong and Wong[3] used polarization and anisotropy patterns backed up by calculations from a spin Hamiltonian that commutes with the group operators. In Fong's more recent collaboration,[4,7] he sees fit to neglect such essential confirmation, relying solely on the form of the anisotropy patterns.

c. C_{2v} patterns. The correct second-order patterns for C_{2v} have been calculated above. There is no first-order effect since there are only one-dimensional representations in C_{2v}. The first-order pattern for "axial" C_{2v} given in Fong and Wong[3] arises from a special case of O_h symmetry plus an axial field in the [110] direction which gives $E=0$ in the C_{2v} spin Hamiltonian and produces the degeneracy which gives a first-order Zeeman effect. Fong and his co-workers have taken half of this first-order pattern and presented it as a general C_{2v} pattern. For reasons given above, this half-pattern would never occur, and their use of it is incorrect.

d. Data presentation. The method of presentation of data by Fong and his co-workers appears to be inconsistent and misleading. For example, Fig. 2 of Fong and Bellows[7] shows the lines at 7031.7 Å barely resolved in the magnetic field and indicates a no-field linewidth of 1.2 Å, but in their Fig. 4 they indicate a linewidth of 0.17 Å for both of these lines compared to a separation of 0.8 Å. The sharpest width the authors have ever been able to obtain for this line is 0.34 Å on the plate reproduced in Fig. 4. This makes it difficult to believe that Fong and Bellows obtained the resolution their reported patterns indicate.

IV. EXPERIMENT

The present authors used a superconducting magnet for the second-order Zeeman effect. The magnet was built at UCLA with 5000 ft of T48B wire obtained from Supercon, on an aluminum coil form with $\frac{1}{2}$-in. i.d., 3.53-in. o.d., and 1.5-in. thickness. The coil goes normal at 32 A with a maximum field of 68 kG. Owing to the small i.d., it is impossible to have the optical path perpendicular to the magnetic field with this coil.

However, operating with optical path parallel to H yields interesting information not shown in Fong and Bellows's data. The spectrometer used was a 2.5-m Ebert with a 5×4-in. grating operated at third order. The plate constant was about 1.6 Å/mm and the tested resolving power was about 200 000. Exposure time varied from 5 min to 1 h

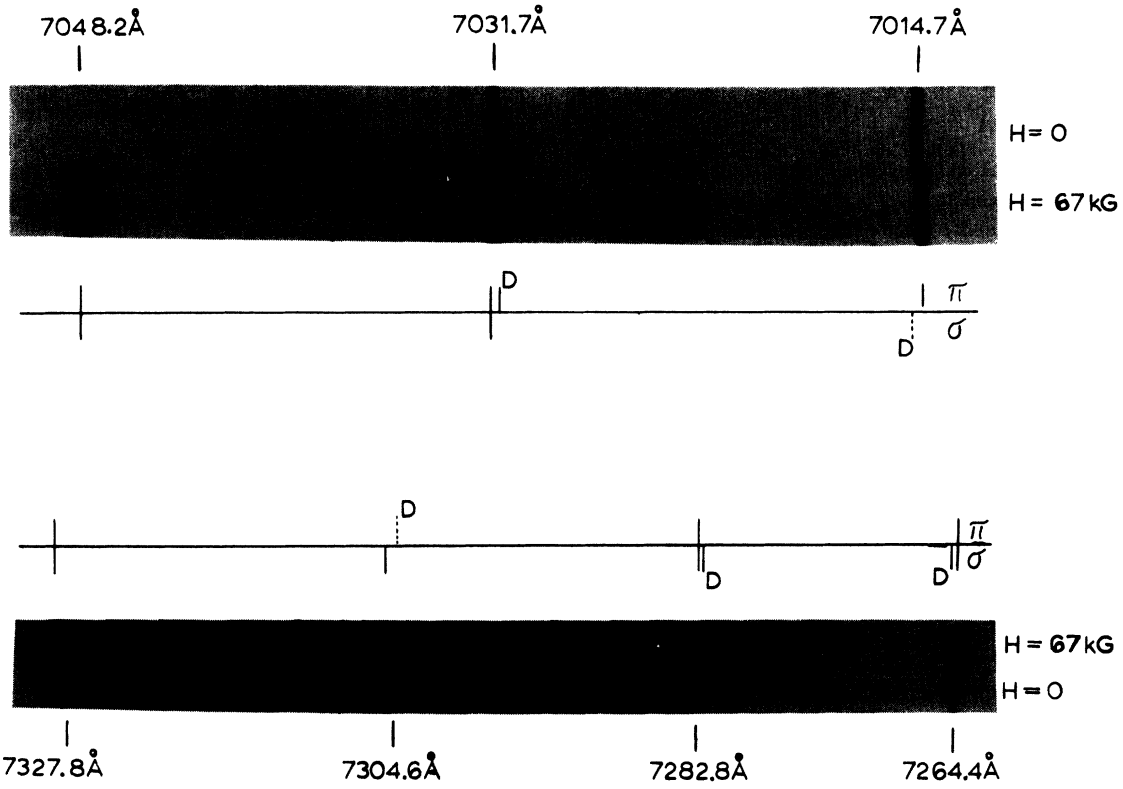

FIG. 4. Zeeman effect in the $^7F_1$ (upper) and $^7F_2$ (lower) regions of the KCl : Sm^{2+} fluorescence spectrum with $\vec{H}$ along [100]. The photographs show the results obtained when observed along the field. The plate taken normal to the field (42 kG) with polarizers was too dim to obtain a good copy, so the results are indicated by the drawings with the appropriate polarizations. The dashed lines mean that these lines are seen when viewed normal to the field (on the polarization plate) but not when viewed along the field (in the photos shown).

depending on the intensity of the lines. The second-order Zeeman effects of the $^7F_1$ and $^7F_2$ groups are shown in Fig. 4.

We decided confirmation by polarization data to be so important that another split-coil magnet was wound with some remaining wire to permit viewing normal to the field. This coil goes normal at 35 A and was operating at a maximum field of 42 kG.

V. DISCUSSION OF RESULTS

Fong and Bellows's intensity data[7] may be used keeping in mind that the photographic plate does not give reliable information if the line is strongly overexposed. Further, the grating spectrometer gives different intensities for $\vec{E}$ orientation parallel and perpendicular to the grating lines. This effect should not be too large for a 2-m Bausch and Lomb in the second order as used by Fong and Bellows. Their densitometer traces will give some idea of the intensity but should be taken seriously only for weak lines.

Identification of Strong Lines

The line at 7014.7 Å has about equal intensity for Fong and Bellows's densitometer trace, and one component is missing in Fig. 4 when viewed along the magnetic field. However, it is the longer-wavelength component which is missing, and this component has been identified as the sites A, B, and C by Fong and Bellows's[7] anisotropy pattern. According to the theory presented above, it is site D which should be missing if the site symmetry is C_{2v}. Either the present theory or Fong and Bellows's pattern is wrong. Site D is missing because the dipole moment is parallel to the observation path. It is hard to believe that all three sites A, B, and C will have dipole moment in the same direction. Further check on this point can be made through the position of the no-field line. According to the calculation given above for the $S = 1$ case, the no-field line should be very close to the line given by site D, and it is indeed the line which is close to the no-field line that is missing. Since the missing line, when viewed perpendicular to the magnetic field, must be π polarized for electric dipole transition and σ polarized for magnetic polarization, the σ polarization of this missing line indicates a magnetic dipole transition and the lower state is

TABLE VI. Decomposition of the ^7F_J levels ($J \leq 2$) of the $4f^6$ configuration under several point-group symmetries.

	O_h	C_{4v}	C_{2v}
$^7F_2$	$\Gamma_{3g}+\Gamma_{5g}$	$\Gamma_1+\Gamma_3+\Gamma_4+\Gamma_5$	$\Gamma_1+\Gamma_3+\Gamma_1+\Gamma_2+\Gamma_4$
$^7F_1$	Γ_{4g}	$\Gamma_2+\Gamma_5$	$\Gamma_2+\Gamma_3+\Gamma_4$
$^7F_0$	Γ_{1g}	Γ_1	Γ_1

a Γ_2.

The possibility of a mistake in Fong and Bellows's pattern should be mentioned here. There are three magnetically different sites when the magnetic field is along the [110] direction or $\theta = 45°$, but only two of the sites are observable. The third site has its oscillating dipole along the observation path. For this reason it is rather doubtful that Fong and Bellows can observe all three components as indicated in their pattern. If the longer-wavelength component at 45°, 37.5°, and 52.5° is a mistake, then their data will agree with our result. This component was searched for by the authors with magnetic fields up to 67 kG without any result. Our result is given in Fig. 5.

The line at 7031.7 Å displays strong and weak components in Fong and Bellows's densitometer trace and shows equal intensity in Fig. 4 of the present work, in agreement with the theory for C_{2v} symmetry. As shown in Fig. 4, the weak component (corresponding to site D) shows σ polarization and the strong component (corresponding to sites A, B, and C) shows σ and π polarization. As seen in Table V, these data are compatible with the assignment of the 7031.7-Å line as a magnetic dipole transition (from Γ_1) to either a Γ_3 or Γ_4 state in C_{2v} site symmetry. Objections to Fong and Bellows's treatment of this line have been mentioned above.

Since the magnetic dipole transition from $^5D_0$ to $^7F_1$ will give equal intensity for all three Stark components of $^7F_1$ under C_{2v} symmetry, the remaining strong line at 7048.2 Å must be the remaining Stark component of $^7F_1$.

The strong line at 7264.4 Å of the $^7F_2$ group was identified by Fong and Bellows as C_{2v} site symmetry, and the present authors agree with this identification. It is difficult to say anything about Fong and Bellows's intensity because this line was overexposed. The equal intensity for both components in Fig. 4 indicates either Γ_1 or Γ_2 lower state. The polarization data support this identification.

The next line at 7282.8 Å was identified by Fong and Bellows as originating from the C_{4v} site. If this line belongs to the C_{4v} site, it must have a Γ_2 as lower state (the $J = 2$ level does not contain Γ_2), and Fong and Bellows should have observed equal intensity for both components while the present authors would have one line missing. The experimental data show an intensity ratio of about 2:1 for Fong and Bellows's densitometer trace and about equal intensity for both components in Fig. 4. This is in complete agreement with C_{2v} symmetry, and the lower state is either a Γ_1 or a Γ_2. The polarization data shown in Fig. 4 are also in agreement.

The broad line at 7304.6 Å shows equal intensity for both components in Fong and Bellows's work. and one line is missing in Fig. 4 of the present work. This could be a Γ_2 of C_{4v} site as identified by Fong and Bellows, except the $J = 2$ level does not contain Γ_2 under C_{4v} symmetry. Most likely Bron and co-workers are right again in their C_{2v} identification, and the lower state is Γ_4. The polarization data support both the C_{4v} and C_{2v} identifications.

The broad line at 7327.8 Å shows no structure, and it is impossible to identify this line except that $^7F_2$ will have four allowed electric dipole transitions under C_{2v} symmetry, and this line must be the remaining transition.

Identification of Weak Lines

The two no-field lines at 7018.0 and 7022.7 Å show more or less symmetrical patterns in Fong and Bellows's work and are sharp enough for the authors to obtain a reliable pattern. The present authors agree quite well on the pattern published by Fong and Bellows, except that at 30° the line at about 7023 Å was missing for reasons unknown to the present authors. Based on the magnetic data, it is possible that this pair of transitions belongs to the $M_J = \pm 1$ state of $^7F_1$ under C_s symmetry.

The weak lines in the $^7F_2$ group are identified as C_{4v} site (except the line at 7263.2 Å) by Fong and Bellows. The authors think this wrong because $J = 2$ does not contain the Γ_2 state under C_{4v} symmetry. The exposure of the polarization plate was too dim to yield any useful information on the weak lines.

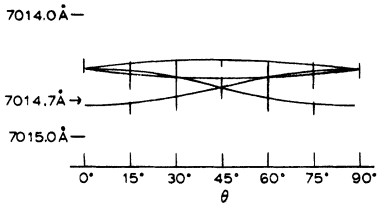

FIG. 5. Zeeman effect obtained for the no-field line at 7014.7 Å with $H = 67$ kG, rotating in the (001) plane, and observation along field. The pattern shown was calculated in the same manner as the patterns in Fig. 2 but includes second-order contributions from the $J = 0$ and $J = 2$ manifolds.

Selective Excitation Experiment

One of the assumptions used here is that the $^5D_0$ state has equal population for all sites. This is not true if the method of excitation is selective. Bron and Heller[1] used selective excitation to identify the lines, and their data should be mentioned here. Their results are listed in column 13 of their Table II, and they are in complete agreement with the present authors' identifications here except for the line at 7282.8 Å of the $^7F_2$ group. The authors believe Bron and Heller made a mistake when they identified this line as magnetic dipole transition. The selection rule for magnetic dipole is $\Delta J = 0$ or ± 1. Magnetic dipole transition from $^5D_0$ to $^7F_2$ is expected to be very weak. If this line is an electric dipole transition, it is in agreement with the present work.

VI. CONCLUSIONS

There is insufficient experimental justification in the Zeeman anisotropy patterns for assigning different site symmetry origins for the prominent lines in the $J < 3$ region of KCl: Sm^{2+} fluorescence spectrum, and the evidence presented here is strongly in favor of a C_{2v} site, most likely nearest neighbor, being responsible for these lines. Neither among the prominent lines nor the weaker lines in this region is there any evidence of C_{4v} site origins. Without supporting information such as polarization, intensity, and calculation from a Hamiltonian, the Zeeman anisotropy patterns cannot be used to make reliable identification of the site symmetry.

Other evidence for the strong lines belonging to the same C_{2v} site can be obtained through relative-intensity and relaxation-time measurements. These methods were carried out by the authors and they are in agreement with the present work. The details are reported in Paper III following.

ACKNOWLEDGMENT

The authors wish to express their gratitude to F. K. Fong for making preprints of his publications available.

*Work supported in part by National Science Foundation Grant No. GP-6183.

[1] W. E. Bron and W. R. Heller, Phys. Rev. 136, A1433 (1964).
[2] P. P. Feofilov, *The Physical Basis of Polarized Emission* (Consultants Bureau, New York, 1961).
[3] F. K. Fong and E. Y. Wong, Phys. Rev. 162, 348 (1967).
[4] F. K. Fong, Phys. Rev. B 1, 4157 (1970).
[5] R. E. Bradbury and E. Y. Wong, preceding paper, Phys. Rev. B 4, 694 (1971).
[6] F. K. Fong, Phys. Rev. 187, 1099 (1969).
[7] F. K. Fong and J. C. Bellows, Phys. Rev. B 2, 2636 (1970).

PHYSICAL REVIEW B VOLUME 4, NUMBER 3 1 AUGUST 1971

Fluorescent Spectra of Sm^{2+} in KCl. III. Site-Symmetry Correlation of Lines by Crystal Comparison and the Thermal Dependence of Intensities and Lifetimes*

R. E. Bradbury and E. Y. Wong
Department of Physics, University of California, Los Angeles, California 90024
(Received 26 October 1970)

In this final paper in the series on the fluorescent spectra of Sm^{2+} in KCl, the authors present results of studies on the spectra of two different crystals at different temperatures, together with detailed studies in one crystal of the intensity and lifetime behavior versus temperature. Three sets of lines are found corresponding to three different site symmetries for the Sm^{2+}–K^+-vacancy system. All the prominent lines belong to the same set showing that they originate from the same level of the same (site-symmetry) ion. Magnetic studies presented in Papers I and II show that this site symmetry is C_{2v}, in accord with the earlier work of Bron and Heller.

I. INTRODUCTION

The charge compensation of divalent cations doped in alkali halides is generally accomplished by an alkali-ion vacancy, with the divalent ion located at an alkali-ion site of the normal lattice. The imperfect nature of the charge compensation can lead to distortions of the normal lattice, particularly if the vacancy is close to the impurity. The location of the vacancy with respect to the impurity will induce symmetries at the impurity ion site which are lower than the corresponding symmetry of the host lattice.

The case of Sm^{2+} in KCl has been of particular

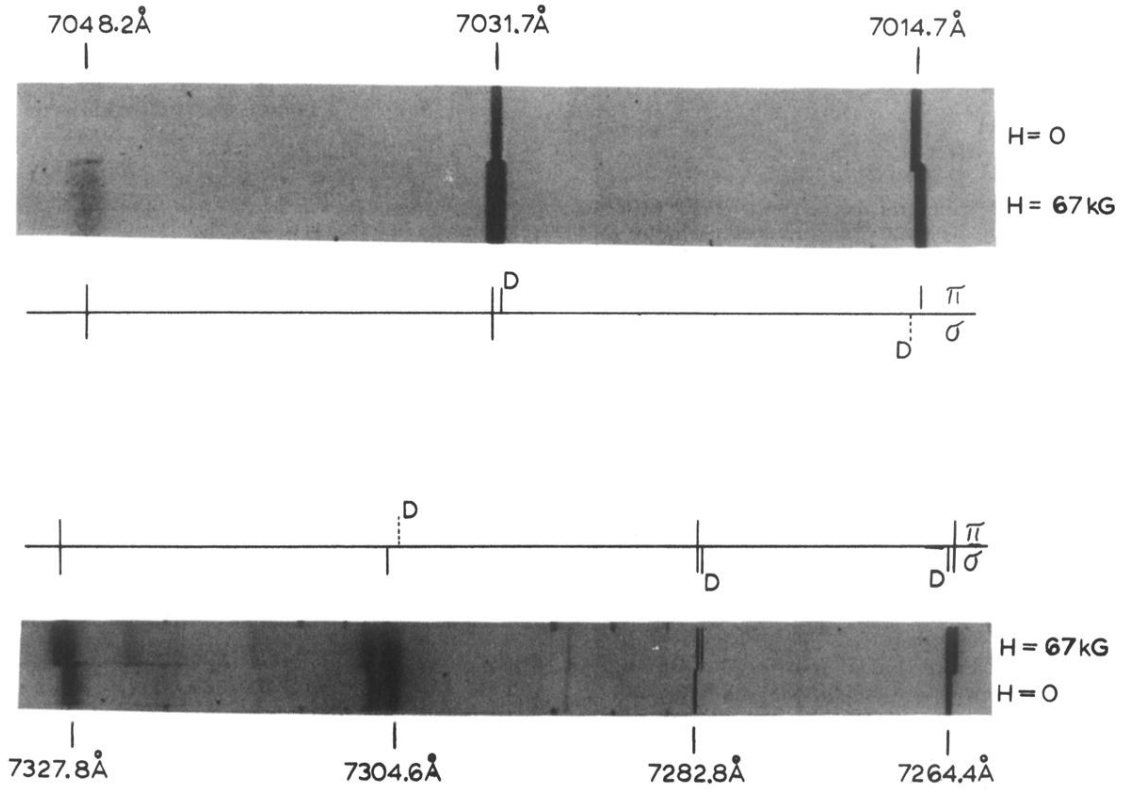

FIG. 4. Zeeman effect in the $^7F_1$ (upper) and $^7F_2$ (lower) regions of the KCl : Sm^{2+} fluorescence spectrum with $\vec{H}$ along [100]. The photographs show the results obtained when observed along the field. The plate taken normal to the field (42 kG) with polarizers was too dim to obtain a good copy, so the results are indicated by the drawings with the appropriate polarizations. The dashed lines mean that these lines are seen when viewed normal to the field (on the polarization plate) but not when viewed along the field (in the photos shown).